A&A, 705, A129 (2026)
https://doi.org/10.1051/0004-6361/202556070
© The Authors 2026

Astronomy & Astrophysics

The interpretation of XRISM X-ray measurements of turbulence in the intracluster medium: A comparison with cosmological simulations

F. Vazza[1,2,⋆] and G. Brunetti[2]

[1] Dipartimento di Fisica e Astronomia, Università di Bologna, Via Gobetti 92/3, 40121 Bologna, Italy
[2] Istituto di Radio Astronomia, INAF, Via Gobetti 101, 40121 Bologna, Italy

Received 24 June 2025 / Accepted 20 November 2025

ABSTRACT

We investigate whether the properties of turbulent gas motions recently measured via X-ray spectroscopy in the Coma cluster of galaxies by XRISM are in tension with the turbulent picture established by current numerical cosmological simulations. We use a high-resolution simulation of a Coma-like cluster and show that the simulation yields velocity structure functions and X-ray line-widths that are compatible with those measured by the XRISM observations of Coma. In particular, it has previously been suggested that a much steeper turbulence spectrum than Kolmogorov's would be needed to explain the XRISM observations under a homogeneous, cluster volume-filling turbulence model. Our results show that this tension is overcome thanks to the more complicated turbulent picture in cosmological simulations, which indeed shows a patchy distribution of turbulent regions in galaxy clusters, with a spectrum that is generally consistent with a Kolmogorov power law over a fairly wide range of scales. More generally, our study highlights the fact that the interpretation of XRISM data of galaxy clusters depends on the turbulence model used and the importance of combining data and advanced simulations in the future steps.

Key words. hydrodynamics – turbulence – large-scale structure of Universe – X-rays: galaxies: clusters

1. Introduction

Turbulence in the intracluster medium (ICM) is expected to arise from the stirring associated with the mass growth of clusters (e.g. Norman & Bryan 1999; Subramanian et al. 2006), and may provide pressure support in the atmosphere of clusters of galaxies (e.g. Brunetti et al. 2001; Petrosian 2001; Fusco-Femiano & Lapi 2013; Biffi et al. 2016; Eckert et al. 2019). Turbulence may also play a role in the origin of non-thermal components in the ICM, leading to the amplification of magnetic fields (e.g. Dolag et al. 1999; Schekochihin et al. 2005; Cho 2014; Beresnyak & Miniati 2016) and to the re-acceleration of relativistic particles (e.g. Brunetti et al. 2004; Cassano & Brunetti 2005; Miniati 2015; Brunetti & Lazarian 2016; Beduzzi et al. 2024; Nishiwaki et al. 2024). The turbulence in clusters of galaxies has been studied for a long time with cosmological hydrodynamical simulations (e.g. Norman & Bryan 1999; Dolag et al. 2005; Iapichino & Niemeyer 2008; Vazza et al. 2011; Miniati 2014), albeit its precise determination depends on the specific algorithms used to filter out bulk motions, shocks, and other perturbations from the three-dimensional velocity field (e.g. see discussion in Vazza et al. 2012; Nelson et al. 2014; Vazza et al. 2017, 2018a; Angelinelli et al. 2020; Vallés-Pérez et al. 2021).

The observed fluctuations of thermodynamic quantities derived from X-rays and from the Sunyaev-Zeldovich effect in clusters of galaxies were interpreted as indications of moderate fluctuations induced by turbulence (e.g. Schuecker et al. 2004; Churazov et al. 2012; Gaspari & Churazov 2013; Zhuravleva et al. 2012; Khatri & Gaspari 2016; Eckert et al. 2017; Dupourqué et al. 2024; Lovisari et al. 2024). Additionally, recent works also analysed the trails of ionised interstellar medium swept up behind 'jellyfish' galaxies to trace turbulence of the surrounding ICM, and inferred the presence of ∼20−100 km/s on 1−60 kpc scales, with a distribution compatible with Kolmogorov turbulence (Li et al. 2023; Ignesti et al. 2024).

However, the direct measurement of turbulence in the ICM has only since recently become possible, with spectroscopic X-ray observations of a few clusters. The Hitomi satellite managed to detect root-mean-square velocities in the (fairly relaxed) Perseus cluster of ∼200 km/s on ≤60 kpc (e.g. Hitomi Collaboration 2016; ZuHone et al. 2018). More recently, the XRISM collaboration reported first measurements of bulk velocity and of the velocity dispersion along a few lines of sight (LOSs) crossing three galaxy clusters in the local Universe: A2029 (Xrism Collaboration 2025a), Coma (Xrism Collaboration 2025b), and Centaurus (XRISM Collaboration 2025). In all cases, the reported values of LOS velocity dispersion (once converted into three-dimensional values, assuming isotropic velocity distributions) are in the ∼200−400 km/s range at all radii, resulting in typical inferred kinetic to total pressure support of ∼2−3%, naively resulting in a much smaller estimate than in previous simulations. A key finding obtained by XRISM in the case of the Coma cluster (a massive perturbed system hosting multiple diffuse radio emissions, Bonafede et al. 2021 for recent observations) is that, while the slope of the velocity structure function (VSF) that they derive from observations is poorly constrained, the combination of the VSF and line broadening requires a turbulent spectrum that is

⋆ Corresponding author: franco.vazza2@unibo.it

Open Access article, published by EDP Sciences, under the terms of the Creative Commons Attribution License (https://creativecommons.org/licenses/by/4.0), which permits unrestricted use, distribution, and reproduction in any medium, provided the original work is properly cited.
This article is published in open access under the Subscribe to Open model. Subscribe to A&A to support open access publication.

much steeper than a Kolmogorov, if a homogeneous turbulent model is assumed (see Eckert et al. 2025, for an updated discussion). This is used to propose either a very large effective viscosity in the ICM inducing a large dissipation scale of turbulent motions, or a situation where large scale motions generated by recent mergers have not yet cascaded down to small scales (Xrism Collaboration 2025b). If confirmed, these findings would start providing fundamental insights into the properties of turbulence in the ICM and on the role of collisionless effects. Indeed, in a weakly collisional plasma instabilities driven by large-scale motions may govern the effective viscosity of the plasma and the fraction of the energy that is drained from large scales into small-scale turbulence (e.g. Kunz et al. 2011; Brunetti & Lazarian 2011; Rincon et al. 2016; St-Onge & Kunz 2018; St-Onge et al. 2020; Kempf & Rincon 2025).

Given the potential impact of these findings, in this article we attempt to explore how effective the current XRISM measurements really are in obtaining constraints on the turbulence in the ICM and whether they are really in tension with current cosmological simulations, which are based on a purely collisional model of the ICM. The paper is structured as follows: in Sect. 2 we describe our simulation; in Sect. 3 we give our results; and in Sect. 4 we discuss the implications of this work for the interpretation of existing and future observations.

2. Methods

We analysed a high-resolution cluster simulation obtained with the Eulerian code ENZO (Bryan et al. 2014), already used in previous work (e.g. Vazza et al. 2018b; Domínguez-Fernández et al. 2019; Bonafede et al. 2021). This ideal magneto-hydrodynamic (MHD) simulation used up to eight levels of adaptive mesh refinement (AMR) to reach a peak spatial resolution of $\Delta x = 3.95\,\mathrm{kpc/cell}$ in most of the cluster core, and a resolution of $\Delta x = 15.8\,\mathrm{kpc/cell}$ in the entire virial volume (Vazza et al. 2018b). We selected this particular cluster simulation because its final mass is close to the one of the real Coma ($M_{200} \approx 1.1 \cdot 10^{15}\,M_{\odot}$ at $z = 0.02$). This system has thermal properties that are very similar to the real Coma in terms of entropy and density profiles (see e.g. Vazza et al. 2010 and also Appendix A). This cluster accreted ~50% of its final virial mass during a major merger (i.e. a mass ratio larger than one fifth of the cluster mass at that time) at around $z \sim 0.45$ (Vazza et al. 2010), and it has ongoing accretion from smaller clumps at $z = 0$, which induce gas perturbation and peripheral shocks, as in the real Coma (e.g. Churazov et al. 2023). We studied this system already to compare with observations of non-thermal properties of the Coma cluster, showing that the simulation produces a Faraday rotation profile consistent with that measured in the Coma cluster (Vazza et al. 2018b) and that the turbulence generated in the simulation allows one to reproduce the observed radio halo under the assumption of second-order acceleration of relativistic electrons (Bonafede et al. 2021). These radio observables are tightly linked with the level of turbulent gas motions naturally developed by major and minor merger events, which we estimated to contribute to ~5% of the total gas pressure in the form of isotropic turbulent motions in the cluster centre (Vazza et al. 2018b).

To compare with recent X-ray observations by the XRISM collaboration, we computed the continuum and line X-ray emission from all cells in the simulation within the [5, 7] keV energy rang, assuming a constant composition and metallicity (30% of the solar one) for all cells, with the B-APEC emission model[1]. For our analysis, we also had to identify the turbulent part of the three-dimensional gas velocity field in the ICM, with a small-scale filtering approach, based on previous work (Vazza et al. 2006, 2009, 2011, 2012, 2017; Angelinelli et al. 2020; Simonte et al. 2022). More sophisticated approaches using a variable filtering length, combined with the masking of velocity jumps induced by shocks, can be used for a more accurate removal of bulk from turbulent motions (Vazza et al. 2012; Angelinelli et al. 2020; Valdarnini 2019). However, we have also shown that the result of such more complex filtering is equivalent to a fixed spatial filtering length with a length of $\Lambda_t \sim R_{100}/10$, i.e. $\Lambda_t \sim 300\,\mathrm{kpc}$ for clusters in the $\sim 10^{15}\,\mathrm{M}_{\odot}$ mass range (see e.g. Vazza et al. 2012, Fig. 6), as bulk motions start to contribute significantly to the gas kinetic energy budget in simulated clusters above this scale (e.g. Vazza et al. 2011, 2017; Angelinelli et al. 2020).

In the remainder of this paper and in line with previous work, we estimated the gas turbulent velocity after filtering out motions on scales $\geq\Lambda_t$: $\delta\boldsymbol{v} = \boldsymbol{v} - \langle\boldsymbol{v}\rangle_{\Lambda_t}$, where $\boldsymbol{v}$ is the local velocity and density and $\langle\boldsymbol{v}\rangle_{\Lambda_t}$ is the velocity averaged on the Λ_t scale. For completeness, we also present results for different fixed filtering lengths: $\Lambda_t = 150, 300, 600$, and $900\,\mathrm{kpc}$. In order to avoid any confusion, in the remainder of the paper we explicitly state when these 'filtered' turbulent velocities are used, while all X-ray weighted quantities (e.g. the velocity dispersion along the LOS) will not include any spatial filtering at all.

3. Results

We show in Fig. 1 maps of the projected X-ray surface brightness obtained in the [5–7] keV band, of the X-ray weighted mean gas temperature, and of the total velocity and velocity dispersion along the LOS. The latter two were computed in two ways: a) in the top panels, by directly computing the average (volume-weighted) velocity and velocity dispersion along each LOS, considering a field of view of $3.95 \times 3.95\,\mathrm{kpc}^2$ for each LOS (as in the original resolution of the simulation), or b) by computing the X-ray emission-weighted average velocity and velocity dispersion along the LOS after resampling on $90 \times 90\,\mathrm{kpc}^2$ pixels (corresponding to a XRISM FOV at the distance of the Coma cluster), similar to Xrism Collaboration (2025b). The figure shows the significant difference between the projection of volume-weighted and X-ray-weighted quantities, with the X-ray-weighted quantities generally biased low, due to the combination of density-squared (X-ray emissivity) weighting, and due to the patchy nature of the turbulence and bulk motions in the simulation. Xrism Collaboration (2025b) recently concluded that the turbulent spectrum in the Coma cluster may be much steeper than Kolmogorov's model of turbulence. This conclusion is motivated by the fact that a Kolmogorov model fitting their measured VSF[2] would predict a line more than twice wider than the measured one. A spectral distribution of velocity fluctuations overall described by the classical $\propto k^{-5/3}$ (where $k = 2\pi/l$ and l is a spatial scale) scaling of Kolmogorov turbulence is instead generally found in all modern cosmological simulations (Dolag et al. 2005; Vazza et al. 2009, 2011, 2017; Simonte et al. 2022).

[1] https://heasarc.gsfc.nasa.gov/xanadu/xspec/manual/Models.html

[2] It will be noticed that the approximately megaparsec-scale point in the VSF of Xrism Collaboration (2025b) has been obtained based on the measured velocity offset between galaxies and the gas distribution, which might be partly contributed to by bulk motions.

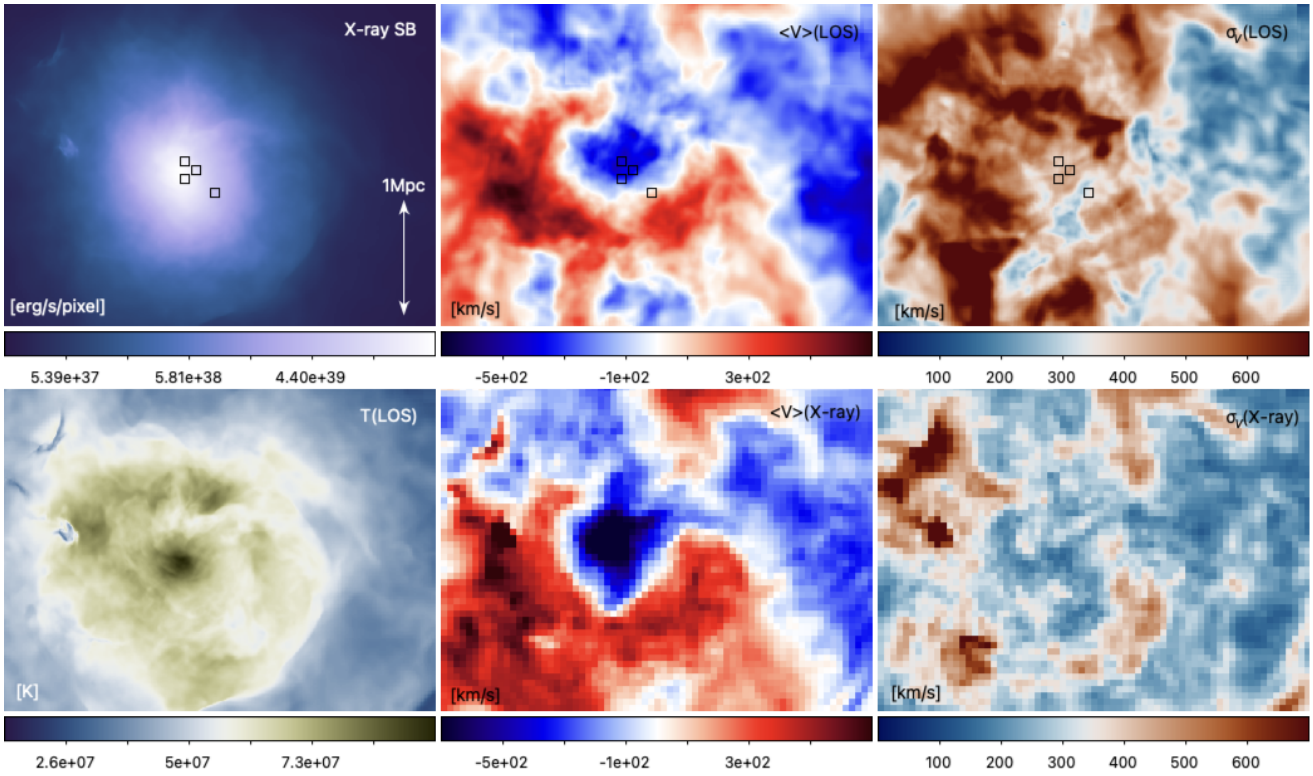

Fig. 1. Projected X-ray surface brightness in the [5–7] keV energy range for our simulated cluster (top left), average X-ray weighted gas temperature (lower left), average gas velocity along the LOS, either using a volume-weighting procedure (top centre) or an X-ray emissivity weighting along the LOS, within pixels of $90 \times 90\,\mathrm{kpc}^2$ to mimic XRISM's field of view for Coma (bottom centre). Gas velocity dispersion along the LOS, again either using a volume-weighting procedure (top right) or an X-ray emissivity weighting along the LOS, for $90 \times 90\,\mathrm{kpc}^2$ pixels (bottom right). The black squares refer to the regions used to produce the line emission profiles given in Fig. 3.

The VSF is defined as $VSF(\boldsymbol{r}) = \langle|\boldsymbol{v}_z(\boldsymbol{\chi}) - \boldsymbol{v}_z(\boldsymbol{\chi} + \boldsymbol{r})|^2\rangle$, where $\boldsymbol{v}_z$ is the velocity along the LOS and $\boldsymbol{r}$ is a displacement with respect to the $\boldsymbol{\chi}$ position. The Kolmogorov model predicts a $VSF(r) \propto r^{2/3}$ scaling for isotropic and volume-filling turbulence. The intrepretation by Xrism Collaboration (2025b) is based on the assumption of a homogeneous turbulent model cluster-volume filling, normalised to the VSF, which is used in combination with the beta-model thermal-density distribution of the Coma cluster to calculate the line width integrated along the LOS (e.g. see also Eckert et al. 2025). Our simulation allows us to step beyond this simplified model and to compare XRISM observations with the properties of turbulence in our simulated Coma-like cluster.

Figure 2 gives the three-dimensional VSF for the velocity component along the LOS, computed from 10^7 cells in the cluster volume. In line with previous work (e.g. Vazza et al. 2011, 2017; Simonte et al. 2022), for more than one order of magnitude in spatial scales the measured VSF is in line with the Kolmogorov model ($\propto r^{2/3}$)[3]. To mimic the recent XRISM analysis of Coma, we produced 50 random variations of the two-dimensional estimates of the VSF, based on the X-ray weighted velocity map with $90 \times 90\,\mathrm{kpc}^2$ pixels (as in the last column of

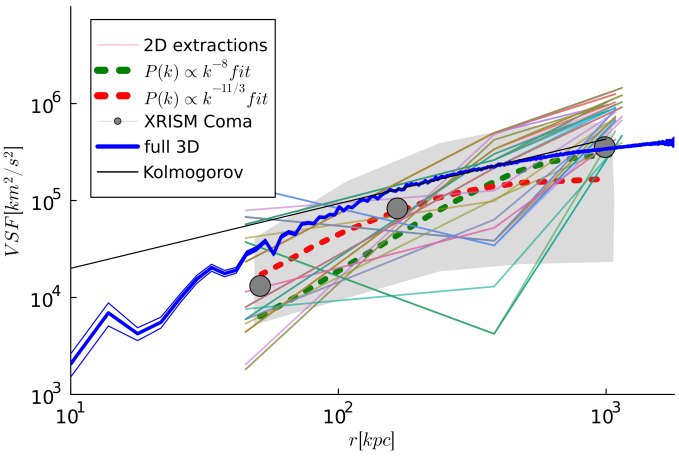

Fig. 2. Thin lines with different colours: simulated VSFs for 50 random LOSs, with an area of $90 \times 90\,\mathrm{kpc}^2$, randomly extracted from our two-dimensional velocity map and with separations as in the XRISM observation of Coma. Blue lines: Full three-dimensional VSF for the velocity along the LOS component, using 10^7 cells in the cluster volume. The grey points are the XRISM measurements for Coma. The additional dashed lines show the best-fit models derived Xrism Collaboration (2025b) for a Kolmogorov spectrum (red) or a much steeper one (green), while the shaded grey area shows the 68% cosmic variance uncertainty and the measurement statistical errors in the same work.

[3] The gas velocity power spectra in clusters of galaxies simulated in cosmology is known to have a steepening, compared to the $\propto k^{-5/3}$, for $\leq$100 kpc scales. This is partially due to numerical effects: velocity fluctuations on scales smaller than $\leq$8 grid cells are increasingly damped by numerical dissipation (e.g. Porter & Woodward 1994; Kritsuk et al. 2011; Miniati 2014). Moreover, AMR additionally reduces the amount of small-scale velocity fluctuations, when spectra or VSFs are computed over a large volumes, owing to the mixing of different AMR levels (e.g. Vazza et al. 2011). Finally, global power spectra of gas motions across the cluster volume are steeper than the ones measured in smaller sub-volumes (which are closer to $\propto k^{-5/3}$), as global spectra mix different turbulent cascades with different normalisations (e.g. Simonte et al. 2022).

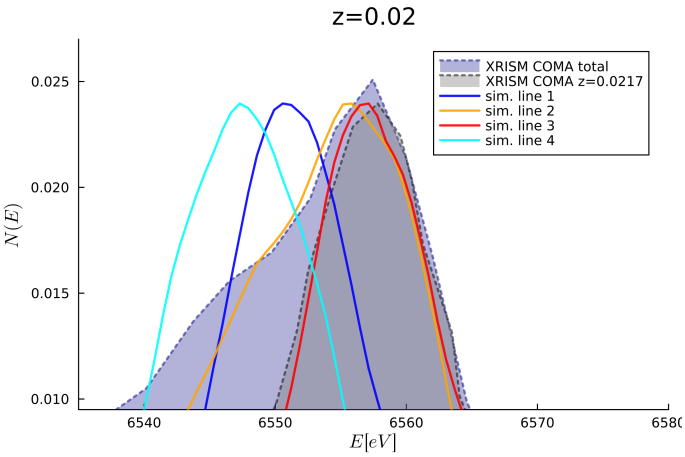

Fig. 3. Simulated line profiles for the four FOVs indicated in Fig. 1 (colour lines) compared with the reconstructed line models for the XRISM observation of the Coma cluster produced by Xrism Collaboration (2025b), given by the two shaded areas.

Fig. 1). In detail, we used triplets of random pixels with a relative projected distance as in the real observation, and we built their VSF by computing the velocity difference between them. The results are shown by the multitude of thin coloured lines (some of which producing even inverted trends of the VSF with increasing scale) in Fig. 2, which are over-imposed to the actual XRISM data point (grey points), to the two models with different slopes discussed in Xrism Collaboration (2025b) and with the region of uncertainties of the VSF discussed there. Within the large scattered distribution of randomly measured VSFs, a large fraction of them are similar to the recent XRISM measurement, and within their estimated statistical uncertainty and cosmic variance. We conclude that our simulated Coma-like cluster is characterised by a three-dimensional velocity field that is compatible with a Kolmogorov turbulence in a stratified medium across a fairly large range of scales, and that its observable VSFs are in principle compatible with the measurements recently made with XRISM.

Next, we show that the same simulated velocity field also appears capable of reproducing the iron line emission measured by XRISM. In detail, we simulated the iron line emission from four lines randomly drawn within a ≤200 kpc region from the cluster centre (whose position is shown by the black squares in Fig. 1), as is shown in Fig. 3. The line emission profile was generated by adding the X-ray emission in the [5–7] keV band for each cell along the LOS (assuming a constant metallicity) and by including the $\Delta E/E = v_z/c$ Doppler shift of the line centre, based on the measured velocity along the LOS (again for $90 \times 90\,\mathrm{kpc}^2$ FOV). The additional shaded areas show the best models produced to fit the north-west quadrant of the XRISM observation of Coma, which plausibly includes a bulk motion along the LOS. Our simulated FOVs generate line shapes with a range of profiles, including cases that closely match the iron line profile measured by XRISM on Coma (such as line 3 for the $z = 0.0217$ component in the Coma observation, or line 2 for the additional velocity component detected by XRISM along the LOS), while other have different shapes (e.g. lines 1 and 4).

This might seem at odds with the conclusions in Xrism Collaboration (2025b), where a Kolmogorov model matching the observed VSF results in a line width that is too large compared to observations. The discrepancy arises from the fact that the turbulence in simulations is very different from a homogeneous and cluster-volume filling model assumed in Xrism Collaboration (2025b). Turbulence in galaxy clusters is driven by several accretion and merging events on different spatial- and time-scales. This generates a number of active turbulent regions with different turbulent intensities that might also mix due to turbulent diffusion and advection. This situation generates an intermittent, multi-scale, and spatially patchy distribution of turbulence with a Kolmogorov-like spectrum across a fairly large range of scales (e.g. Dolag et al. 2005; Iapichino & Niemeyer 2008; Vazza et al. 2009, 2011; Miniati 2014). As a net result, we find that the effective line width in this situation is reduced by a factor of ∼2 compared to that estimated from a homogeneous and cluster-volume filling model with the same turbulent energy budget and spectrum (Appendix B).

We also remark that this result appears in line with the test shown in the appendix of Xrism Collaboration (2025b), where the emission-weighted velocity dispersion for 14 Coma-like clusters is measured. In light of these results, another important point is to evaluate the fairness of the turbulence energy budget estimated from the integrated line-width along the LOS. Given the complex properties of turbulence in the simulated clusters, it is not immediately clear which fluctuation scales the XRISM measurements are sensitive to, and what biases arise from emissivity weighting in the inhomogeneous and stratified ICM. The top panel of Fig. 4 gives the distribution of the X-ray weighted velocity dispersion (unfiltered) and of the distribution of 'true' turbulence along the LOS (which is based on our fiducial three-dimensional small-scale filtering procedure for $\Lambda_t = 300\,\mathrm{kpc}$), while the central panel gives the ratio between the two within each $90 \times 90\,\mathrm{kpc}^2$ LOSs. In both cases we consider only central (≤500 kpc from the cluster centre) regions. While the distribution of the X-ray velocity dispersion is well within the estimates recently produced by Xrism Collaboration (2025b), the distribution of our best estimate of the true (filtered) turbulent content in the same cluster is higher on average, typically by ∼40−50% (at a ∼200−300 kpc radius). The lower panel gives the ratio between the X-ray weighted and the turbulent velocity dispersion as a function of the X-ray emission within FOV: the ratio on average decreases as a function of increasing X-ray surface brightness, albeit with a significant scatter that prevents one from extracting a simple correction factor, because the mismatch does not only depend on the X-ray surface brightness, but rather on the specific gas structures along the LOS.

Finally, we re-assessed the amount of the non-thermal pressure support in this cluster, to closely compared with the result by Xrism Collaboration (2025b), who reported a kinetic pressure support of ≈3% of the total pressure in the cluster centre. In Fig. 5 we give the three-dimensional profile of the ratio between turbulent and total pressure within the radius. We used the same formula by Xrism Collaboration (2025b): $p_{\mathrm{turb,kin}}/p_{\mathrm{tot}} = [1 + 3/(\gamma \mathcal{M}^2_{\mathrm{3D}})]^{-1}$, where $\mathcal{M}_{\mathrm{3D}}$ is the local three-dimensional Mach number measured by dividing either the turbulent velocity dispersion or the total velocity dispersion for the sound speed of each cell. Here we show the estimates of the non-thermal pressure support by turbulent motions obtained using four different filtering lengths of increasing size, i.e. from $\Lambda_t = 150\,\mathrm{kpc}$ to =900 kpc (with $\Lambda_t = 300\,\mathrm{kpc}$ being our fiducial choice due to the large contamination by bulk motions on larger scales, as is discussed in Sect. 2). In all cases the non-thermal pressure ratio increases with radius, as was expected (Vazza et al. 2018a), with the total (unfiltered) kinetic pressure reaching ∼30% at large radii, and with the turbulent kinetic pressure ranging from ∼3% to ∼20%, depending on the adopted filtering length. For our fiducial estimate of turbulence in clusters

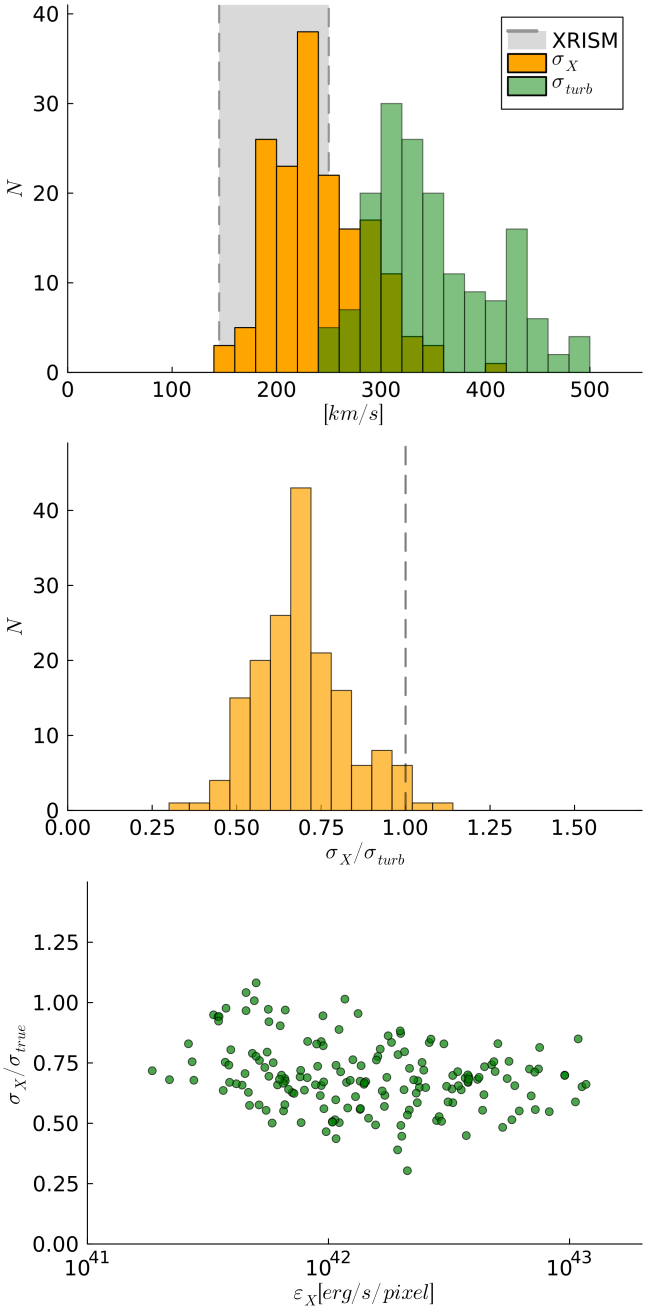

Fig. 4. Top panel: Histograms of X-ray weighted velocity dispersion along the LOS and of volume weighted filtered turbulent velocity dispersion (after the application of our small-scale filtering with a Λ = 300 kpc scale) for 90×90 kpc^2 pixel maps. The additional vertical lines give the values inferred for the central FOVs observed by XRISM in the central region of Coma. Central panel: Histograms for the ratio between the two estimates of the velocity dispersion above. Bottom panel: Ratio between the X-ray weighted velocity dispersion the filtered turbulent velocity dispersion within the Λ = 300 kpc scale, as a function of the X-ray emission of cells.

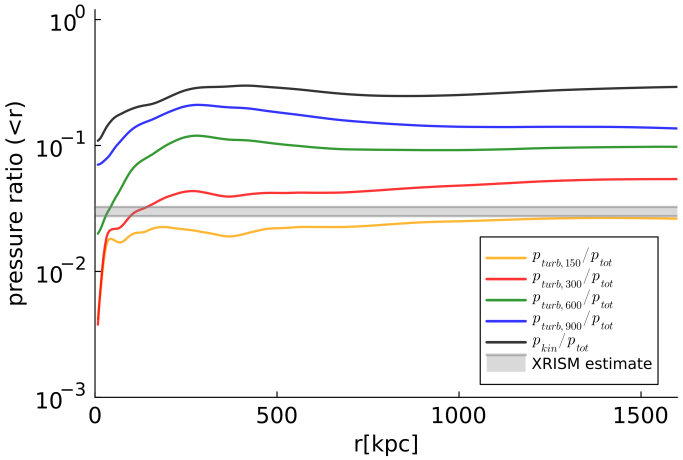

Fig. 5. Three-dimensional radial profile of the non-thermal to total pressure ratio within the radius, considering the total (unfiltered) gas velocity field ($p_{\rm kin}$) or four different choices for the small-scale filtering length (Λ = 150, 300, 600, and 900 kpc, where $p_{\rm turb,300}$ is our reference estimate as discussed in the main text). The horizontal grey strip gives the estimate for the Coma cluster by Xrism Collaboration (2025b).

of this size (Λ_t = 300 kpc), we get ∼5% of non-thermal pressure within 1.5 Mpc from the cluster centre, which is $\approx R_{500}$ for this cluster. This budget is higher than what is estimated for the Coma cluster by Xrism Collaboration (2025b), but is also in line with our previous estimates for this, and similar simulated clusters (e.g. Vazza et al. 2011, 2018b). Based on the relative distribution between X-ray weighted and true turbulence along the LOS, we conclude that actual turbulent non-thermal support in the ICM is significantly higher (typically by a factor ∼2) than the estimate given by spectroscopic X-ray analysis, which is in turn biased low by the smaller range of scales sampled through X-ray emission.

As a final remark, we note that turbulent density fluctuations in the ICM might be constrained also from projected X-ray surface brightness fluctuations (e.g. Gaspari et al. 2014; Zhuravleva et al. 2014; Eckert et al. 2017; Mohapatra et al. 2020, 2021), although the relation between velocity and density fluctuations is more complex in realistic ICM conditions (Simonte et al. 2022, see also the discussion in Xrism Collaboration 2025b). A combined analysis of X-ray surface brightness fluctuations and line broadening generated by our simulations has the potential to further shed light on the properties of turbulence and will be studied with future work.

4. Conclusions

The physics of turbulence in the weakly collisional ICM is expected to be more complicated than that in fluid numerical simulations, where an idealised collisional plasma is assumed. In this article we have investigated whether the recently observed properties of turbulent gas motions inferred via X-ray spectroscopy by Xrism Collaboration (2025b) are already in tension with the idealised view from numerical simulations on large sales (≥10 kpc) and have already started to pinpoint aspects driven by the collisionless nature of the ICM, which are expected to arise on smaller scales (e.g. Kunz et al. 2011; Brunetti & Lazarian 2011; Santos-Lima et al. 2014; Brunetti & Jones 2014; Rincon et al. 2016; St-Onge & Kunz 2018; St-Onge et al. 2020; Kempf & Rincon 2025).

In particular, using a homogeneous and cluster-volume filling model of turbulence, the VSF and X-ray line width measured by XRISM require a turbulent spectrum that is much steeper than a Kolmogorov, possibly pinpointing either a very large effective viscosity in the ICM or a situation in which large-scale motions generated by recent mergers have not yet cascaded down to small scales. Using a high-resolution cosmological simulation of a Coma-like cluster (Sect. 2), we have shown that:

- The spatially patchy, non-homogeneous, and multi-scale turbulence in the simulation generates a VSF and X-ray linewidths integrated along the LOS that are both consistent with the XRISM observations, releasing the request of a turbulent spectrum that is much steeper than a Kolmogorov. This also shows that the interpretation of XRISM data is very sensitive to the assumed turbulent model.
- X-ray lines integrated along the LOS are sensitive to the brightest X-ray regions. This biases the effect of line broadening due to turbulence to an extent that depends on the properties of the turbulence itself in the integrated volume. In our simulation we find that the simulated widths of XRISM X-ray lines are biased low by ∼50% with respect to the turbulent velocity dispersion on scale ∼300 kpc that is measured along the LOS. This bias arises from two factors: the limited range of scales of the turbulent spectrum sampled in this way, and the limited radial extent from the cluster centre that can be probed by X-ray observations (which are biased towards the innermost dense cluster regions).
- The pressure support in our simulated cluster from turbulence on filtered scales of 300–600 kpc is estimated in the range ∼5−10%, which is ∼2−3 times larger than that estimated from the widths of X-ray lines obtained from the simulation, which are consistent with those measured by Xrism Collaboration (2025b). The actual turbulent pressure support in the ICM can plausibly be higher than what is estimated from X-ray spectroscopy, although it is not possible to derive a simple correction factor, due to the large measured scatter in the relation between the true and the X-ray weighted turbulent dispersion along the LOS (see also, e.g. Roncarelli et al. 2018; Biffi et al. 2022; Lebeau et al. 2025, or valuable numerical work on this issue).

In summary, we suggest that the fluid turbulence typically produced by cosmological simulations of galaxy clusters (including our ones and the majority of those in the literature) is compatible with the latest XRISM measurements in Coma, and possibly in other clusters, provided that the realistic degree of non-homogeneity of the ICM, the multi-scale nature of the ICM turbulent flows, and the biases inherent to X-ray spectroscopy are fully taken into account. More in general, our results highlights the importance of advanced numerical simulations to support the interpretation of the data from X-ray calorimeters in the future.

Acknowledgements. FV has been partially supported by Fondazione Cariplo and Fondazione CDP, through grant n° Rif: 2022–2088 CUP J33C22004310003 for the "BREAKTHRU" project. GB acknowledges partial support from INAF Theory Grant "Theory and simulations of non-thermal phenomena in galaxy clusters and beyond". F.V. acknowledges the CINECA award "IscrB_CREW" under the ISCRA initiative, for the availability of high-performance computing resources and support. We also acknowledge the usage of online storage tools kindly provided by the INAF Astronomical Archive (IA2) initiative (http://www.ia2.inaf.it). We wish to thank our reviewer for the valuable comments on our draft, and S. Ettori, D. Eckert, T. Lebeau, A. Ignesti, F. Rincon, M. Markevitch, V. Biffi, J. Zuhone and I. Zhuravleva for helpful comments and discussons. The authors wish to declare that 0% of their original manuscript has been produced using AI of any sort.

References

Angelinelli, M., Vazza, F., Giocoli, C., et al. 2020, MNRAS, 495, 864
Beduzzi, L., Vazza, F., Cuciti, V., et al. 2024, A&A, 690, A67
Beresnyak, A., & Miniati, F. 2016, ApJ, 817, 127
Biffi, V., Borgani, S., Murante, G., et al. 2016, ApJ, 827, 112
Biffi, V., ZuHone, J. A., Mroczkowski, T., Bulbul, E., & Forman, W. 2022, A&A, 663, A76
Bonafede, A., Brunetti, G., Vazza, F., et al. 2021, ApJ, 907, 32
Brunetti, G., & Jones, T. W. 2014, Int. J. Mod. Phys. D, 23, 1430007
Brunetti, G., & Lazarian, A. 2011, MNRAS, 412, 817
Brunetti, G., & Lazarian, A. 2016, MNRAS, 458, 2584
Brunetti, G., Setti, G., Feretti, L., & Giovannini, G. 2001, MNRAS, 320, 365
Brunetti, G., Blasi, P., Cassano, R., & Gabici, S. 2004, MNRAS, 350, 1174
Bryan, G. L., Norman, M. L., O'Shea, B. W., et al. 2014, ApJS, 211, 19
Cassano, R., & Brunetti, G. 2005, MNRAS, 357, 1313
Cho, J. 2014, ApJ, 797, 133
Churazov, E., Vikhlinin, A., Zhuravleva, I., et al. 2012, MNRAS, 421, 1123
Churazov, E., Khabibullin, I., Lyskova, N., Sunyaev, R., & Bykov, A. M. 2021, A&A, 651, A41
Churazov, E., Khabibullin, I., Bykov, A. M., Lyskova, N., & Sunyaev, R. 2023, A&A, 670, A156
Dolag, K., Bartelmann, M., & Lesch, H. 1999, A&A, 348, 351
Dolag, K., Vazza, F., Brunetti, G., & Tormen, G. 2005, MNRAS, 364, 753
Domínguez-Fernández, P., Vazza, F., Brüggen, M., & Brunetti, G. 2019, MNRAS, 486, 623
Dupourqué, S., Clerc, N., Pointecouteau, E., et al. 2024, A&A, 687, A58
Eckert, D., Gaspari, M., Vazza, F., et al. 2017, ApJ, 843, L29
Eckert, D., Ghirardini, V., Ettori, S., et al. 2019, A&A, 621, A40
Eckert, D., Markevitch, M., ZuHone, J. A., et al. 2025, A&A, 704, A35
Fusco-Femiano, R., & Lapi, A. 2013, ApJ, 771, 102
Gaspari, M., & Churazov, E. 2013, A&A, 559, A78
Gaspari, M., Churazov, E., Nagai, D., Lau, E. T., & Zhuravleva, I. 2014, A&A, 569, A67
Hitomi Collaboration (Aharonian, F., et al.) 2016, Nature, 535, 117
Iapichino, L., & Niemeyer, J. C. 2008, MNRAS, 388, 1089
Ignesti, A., Brunetti, G., Gullieuszik, M., et al. 2024, ApJ, 977, 219
Kempf, J. M., & Rincon, F. 2025, A&A, 694, A25
Khatri, R., & Gaspari, M. 2016, MNRAS, 463, 655
Kritsuk, A. G., Nordlund, Å., Collins, D., et al. 2011, ApJ, 737, 13
Kunz, M. W., Schekochihin, A. A., Cowley, S. C., Binney, J. J., & Sanders, J. S. 2011, MNRAS, 410, 2446
Lebeau, T., Ettori, S., Sorce, J. G., Aghanim, N., & Paste, J. 2025, A&A, submitted [arXiv:2506.14441]
Li, Y., Luo, R., Fossati, M., Sun, M., & Jáchym, P. 2023, MNRAS, 521, 4785
Lovisari, L., Ettori, S., Rasia, E., et al. 2024, A&A, 682, A45
Miniati, F. 2014, ApJ, 782, 21
Miniati, F. 2015, ApJ, 800, 60
Mohapatra, R., Federrath, C., & Sharma, P. 2020, MNRAS, 493, 5838
Mohapatra, R., Federrath, C., & Sharma, P. 2021, MNRAS, 500, 5072
Nelson, K., Lau, E. T., & Nagai, D. 2014, ApJ, 792, 25
Nishiwaki, K., Brunetti, G., Vazza, F., & Gheller, C. 2024, ApJ, 961, 15
Norman, M. L., & Bryan, G. L. 1999, Lect. Notes Phys., 530, 106
Petrosian, V. 2001, ApJ, 557, 560
Porter, D. H., & Woodward, P. R. 1994, ApJS, 93, 309
Rincon, F., Califano, F., Schekochihin, A. A., & Valentini, F. 2016, Proc. Natl. Acad. Sci., 113, 3950
Roncarelli, M., Gaspari, M., Ettori, S., et al. 2018, A&A, 618, A39
Santos-Lima, R., de Gouveia Dal Pino, E. M., Kowal, G., et al. 2014, ApJ, 781, 84
Schekochihin, A. A., Cowley, S. C., Kulsrud, R. M., Hammett, G. W., & Sharma, P. 2005, ApJ, 629, 139
Schuecker, P., Finoguenov, A., Miniati, F., Böhringer, H., & Briel, U. G. 2004, A&A, 426, 387
Simionescu, A., Werner, N., Urban, O., et al. 2013, ApJ, 775, 4
Simonte, M., Vazza, F., Brighenti, F., et al. 2022, A&A, 658, A149
St-Onge, D. A., & Kunz, M. W. 2018, ApJ, 863, L25
St-Onge, D. A., Kunz, M. W., Squire, J., & Schekochihin, A. A. 2020, J. Plasma Phys., 86, 905860503
Subramanian, K., Shukurov, A., & Haugen, N. E. L. 2006, MNRAS, 366, 1437
Valdarnini, R. 2019, ApJ, 874, 42
Vallés-Pérez, D., Planelles, S., & Quilis, V. 2021, MNRAS, 504, 510
Vazza, F., Tormen, G., Cassano, R., Brunetti, G., & Dolag, K. 2006, MNRAS, 369, L14
Vazza, F., Brunetti, G., Kritsuk, A., et al. 2009, A&A, 504, 33
Vazza, F., Brunetti, G., Gheller, C., & Brunino, R. 2010, New Astron., 15, 695
Vazza, F., Brunetti, G., Gheller, C., Brunino, R., & Brüggen, M. 2011, A&A, 529, A17
Vazza, F., Roediger, E., & Brüggen, M. 2012, A&A, 544, A103
Vazza, F., Jones, T. W., Brüggen, M., et al. 2017, MNRAS, 464, 210
Vazza, F., Angelinelli, M., Jones, T. W., et al. 2018a, MNRAS, 481, L120
Vazza, F., Brunetti, G., Brüggen, M., & Bonafede, A. 2018b, MNRAS, 474, 1672
XRISM Collaboration (Audard, M., et al.) 2025, Nature, 638, 365
Xrism Collaboration (Audard, M., et al.) 2025a, ApJ, 982, L5
Xrism Collaboration (Audard, M., et al.) 2025b, ApJ, 985, L20
Zhuravleva, I., Churazov, E., Kravtsov, A., & Sunyaev, R. 2012, MNRAS, 422, 2712
Zhuravleva, I., Churazov, E. M., Schekochihin, A. A., et al. 2014, ApJ, 788, L13
ZuHone, J. A., Miller, E. D., Bulbul, E., & Zhuravleva, I. 2018, ApJ, 853, 180

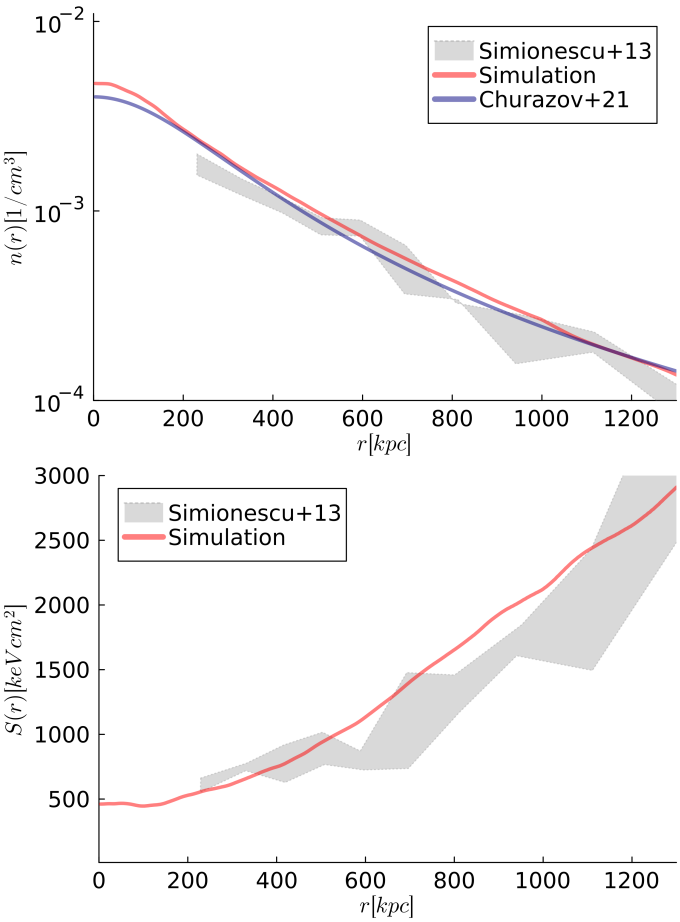

Fig. A.1. Average radial density (top) and gas entropy (bottom) profile for our simulated cluster at $z = 0.02$, compared with recent observational constraints for the real Coma cluster derived by Simionescu et al. (2013) using SUZAKU (the grey areas contain the two measurements taken within two narrow sectors in the outskirts of Coma), and by Churazov et al. (2021) using eROSITA.

Appendix A: Comparison with radial profiles of the Coma cluster

We compared the radial profiles of gas density, $n(r)$ and gas entropy (defined as $S(r) = T(r)/n(r)^{2/3}$ where T is the gas temperature) from our Coma-like simulated cluster, with the available observational constraints for the real Coma. This is shown by the two panels in Fig.A.1. The simulated density profile compares reasonably well with β-model parametrisation recently obtained by Churazov et al. (2021) using X-ray observations by the eROSITA satellite, and also with the pointed deep X-ray exposures of two narrow selections along the E+NE and NW+W directions in the Coma cluster, take by Simionescu et al. (2013) using SUZAKU. The lower panel shows that the average gas entropy profile of our simulated cluster is also fairly in line with the most recent constrains obtained by Simionescu et al. (2013) using SUZAKU. The reasonably good comparison with these two constraints for the real Coma cluster is reassuring as it shows that the gas matter distribution (and its related X-ray emission) from our model is realistic, and also that the entropy stratification of our simulated cluster (which in turns is related to buoyancy and gas mixing as a function of radius) is in line with observations.

Appendix B: Comparison with idealised turbulence

In order to quantify the importance of the turbulent model, here we present the comparison between the line width obtained by integrating the simulation along the LOS and that obtained using a homogeneous and volume filling Kolmogorov turbulent model, similar to the procedure adopted in Xrism Collaboration (2025b) and in Eckert et al. (2025). To calculate the homogenous model, we initialised a spherically symmetric β-model gas density profiles with parameters of the Coma cluster (e.g. Churazov et al. 2021, and references therein) for a 1.6^3Mpc^3 volume using 400^3 cells, and we generated a random 3-dimensional velocity field in Fourier domain, assuming it follows the Kolmogorov scaling ($P(k) \propto k^{-5/3}$) from the largest to the smallest available grid scales. In order to obtain a random Gaussian distribution of velocities, we randomly extracted vectors components from the Rayleigh distribution. The 3-dimensional velocity field within the 1.6^3Mpc^3 volume generated in such a way is renormalised to exactly match the kinetic energy budget, within an equivalent volume centred on the cluster centre, in our cosmological simulation. Figure B.1 shows the distribution of gas density and velocity along the LOS for two middle planes in the two datasets, while Fig. B.2 shows the comparison of the 3-dimensional velocity power spectra of the two datasets. The latter confirms the trend of the VSF of Fig.2: the spectrum of gas motions in the simulated cluster approximately follows the Kolmogorov spectrum up to $\sim$ 1.6 Mpc, while it steepens for $\leq$ 100 kpc scales (see Sect. 3 for a discussion).

In Fig. B.3 we show the distribution of the X-ray weighted gas velocity dispersion along 10^4 random LOSs through the two simulated datasets. The distribution derived from the cosmological simulation of our cluster is clearly peaked at a smaller value, $\sigma_{X,LOS} \sim 180$ km/s, while the distribution derived from the idealised turbulent model peaks at the higher value of $\sigma_{X,LOS} \sim 330$ km/s.

This simple experiment (although limited to the central fraction of the simulated volume, and not to the full depth of the LOSs used in Fig.4) very well illustrates that, for a realistic dynamical model of turbulence in the ICM, a smaller typical broadening of X-ray lines is to be expected, compared to a more idealised model of turbulence, despite the total kinetic energy of the two models is the same. The key factor here is the realistic level of intermittency of turbulence naturally produced by the multi-scale accretions onto cluster simulated in cosmology: turbulence has in this case a smaller filling factor compared to fully homogenous models which assume a large injection scale and stationary driving. For the same total kinetic energy budget, a more intermittent turbulence distribution produces on average a smaller velocity dispersion along the LOS. Conversely, if two models produce on average the same broadening of X-ray lines along the LOS, homogenous model is biased to be characterised by significantly smaller kinetic energy budget. Finally, with an additional test (green line) we show the distribution of X-ray weighted gas velocity dispersions obtained in a "mixed" model, in which we use the β-model density distribution to compute the X-ray emission, and combine this with the 3-dimensional velocity field of the cosmological simulation. The distribution obtained in this way is quite close the one obtained using the density distribution from the simulation, and it shows that the key factor here is the intermittency in the turbulent velocity field, and not in the density field.

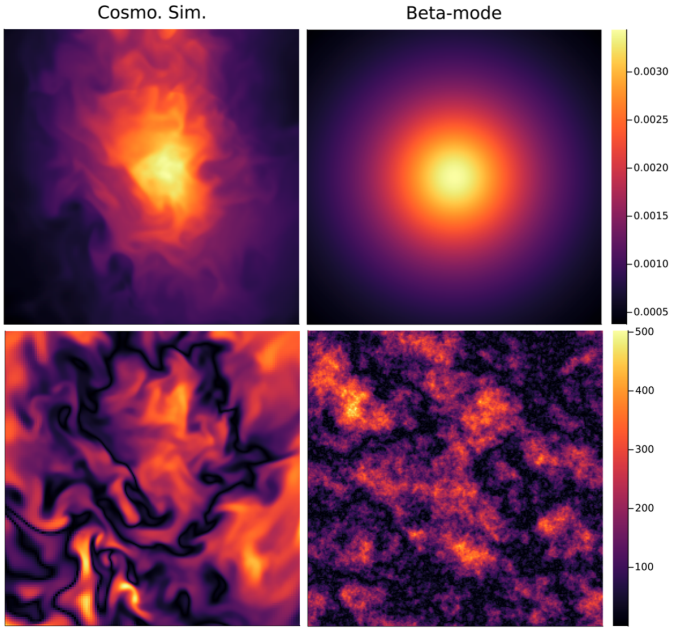

Fig. B.1. Top panels: Central slice showing the distribution of gas density (in units of [part/cm^3]) for the clusters simulation analysed in the main article, and for a β-model of the Coma cluster instead. Lower panels: Distribution of the amplitude of the gas velocity field (in units of [km/s] for the same cosmological simulation (left) or for a 3-dimensional velocity field generated in Fourier space so that it follows the Kolmogorov spectrum for homogenous and stationary turbulence. Each panel has a side 1.6 Mpc.

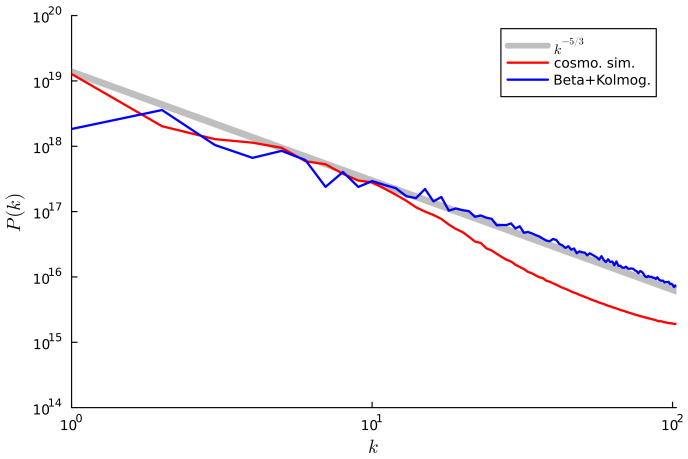

Fig. B.2. Power spectrum (in arbitrary units) of the velocity field for the two cases discussed in Appendix B, with the additional $\propto k^{-5/3}$ shown for comparison.

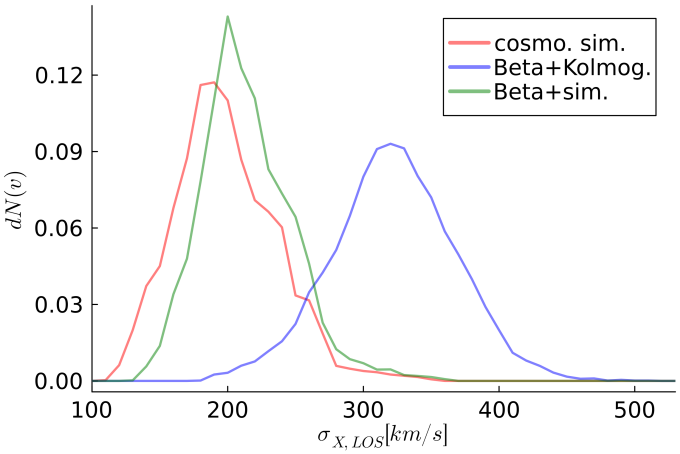

Fig. B.3. Comparison of the distribution of the X-ray weighted gas velocity dispersion along 10^4 simulated LOSs through the three datasets considered in Appendix B: a symmetric β-model distribution of density combined with a homogenous random velocity field (blue), the density and velocity field taken from our cluster simulation (red), and an additional "mixed" model which combines the density distribution of the first model with the velocity field of the second model.